Journal of Engineering Science and Technology
Vol. 15, No. 2 (2020) 1267 - 1276

SIMULATION OF MICRO-RING RESONATOR USING FINITE-DIFFERENCE TIME-DOMAIN TECHNIQUE FOR SENSORS

LILIK HASANAH[1,*], BUDI MULYANTI[2], ROER E. PAWINANTO[2], ASEP B. D. NANDIYANTO[3], YUSKI M. R. FAOZAN[2], ARJUNI B. PANTJAWATI[2], HARBI S. NUGRAHA[1], AHMAD R. MD. ZAIN[4,5], JANULIS P. PURBA[2]

[1]Department of Physics Education, Universitas Pendidikan Indonesia, Jl. Dr. Setiabudi No. 229, 40154, Bandung, Indonesia
[2]Department of Electrical Engineering Education, Universitas Pendidikan Indonesia, Indonesia
[2]Department of Chemistry Education, Universitas Pendidikan Indonesia, Indonesia
[4]Institute of Microengineering and Nanoelectronics, Universiti Kebangsaan Malaysia, 43600, Bangi, Selangor, Malaysia
[5]John A. Paulson, School of Engineering and Applied Sciences, Harvard University, Oxford St, Cambridge, United States
*Corresponding Author: lilikhasanah@upi.edu

Abstract

The purpose of this research was to get the optimum design of materials that can be used as a sensitive sensor. In this study, a micro-ring resonator was used as a model. This resonator was utilized because it is more sensitive in sensing biomolecules than other types of sensors. Two types of micro-ring resonator were simulated: full etching and half etching. To achieve the optimum design of a micro-ring sensor, both models were tested with different dimensions, including waveguide width, gap, ring of radius, and etching depth. These dimensions were evaluated to get the free spectral range (FSR) and quality factor (Q-factor). The high value of FSR indicates sensor sensitivity, whereas Q-factor replies sensor accuracy. We found that both models can obtain the optimum value by providing specific dimensions.

Keywords: Free spectral range, Micro-ring resonator, Quality factor, Sensors.

1. Introduction

Current sensors are needed in large quantities, including physical and chemical sensors. Physical sensors are found in temperature sensors, whereas chemical sensors are found in gas sensors [1]. However, current sensors have limitations in the deficiencies of the conductivity sensors, corrosion, less sensitiveness, and detection range. Among various chemical sensors, micro-ring resonator for sensor application is the most sensitive. Chenyang explained that their micro-ring resonators were good for increasing the sensitivity of sensors based on wavelength shift measurement [2]. But they did not evaluate the value of FSR.

They only calculated the Q-factor; thus, the sensitivity was quite low. Donzella [3] explained that micro-ring resonator sensors were good for fabricating water sensor and air sensors. However, Donzella's design uses only one straight line; thus, both values of FSR and Q-factor were not high. Wright described that the micro-ring resonator is a good sensor with regard to sensitivity for biological sensing applications [4]. But, the sensor design evaluated only the Q-factor and used one straight line on the micro-ring resonator. Another group of researcher showed that the micro-ring resonator can be used for sensor applications to evaluate the light wavelength signal [5, 6]. However, they did not calculate the values of FSR and Q-factor.

Among several studies, none has focused on the design of the micro-ring resonator sensors, which optimized the values of FSR and Q-factor by adjusting the dimensions. Therefore, the purpose of this study was to simulate the micro-ring resonator and optimize the values of FSR and Q-factor by adjusting the dimensions, which is necessary to enhance the performances of the micro-ring resonator sensors [7]. In this research, we used two models of the micro-ring resonator: Model 1 with a full-etching process and Model 2 with a half-etching process, as shown in Fig. 1. We also evaluated some dimensions of the micro-ring (e.g., the waveguide width, gap, and ring radius) to obtain the high values of FSR and Q-factor.

FSR of the micro-ring resonator in the sensor determines the detection range, and the Q-factor shows the sensor sensitivity [8]. The result of the simulation suggested that both models had optimum FSR and Q-factor values for the best adjustment of micro-ring resonator dimensions. To simulate the shape or model of the micro-ring resonator, we used the software based on the finite-difference time-domain, such as XFDTD, SEMCAD, Rsoft [9], and Lumerical. But in this research, we used the Lumerical software because of the mesh refinement factor in which, the result more accurately since the device structure in a tiny dimension.

Based on the study by Talebifard, the Lumerical software has the ability to produce simulation results, which are close to the experimental results [10]. Therefore, the simulation results in this work are expected to provide the approximation of experimental results. Comparison between the current and previous works was also done to validate the simulation results in this work.

2. Method

In this research, we have investigated different configurations of micro-ring resonator based on silicon on insulator, as shown in Fig. 1. Figure 1(a) shows the configuration of the common type of micro-ring resonator, called Model 1, which

has a fully etched Si layer, except for the waveguides with certain dimensions. While in Fig. 1(b), we propose different configurations of a micro-ring resonator, we called Model 2, which the Si layer besides the waveguides structure is not fully etched to left certain level of Si etching depth (H) above the SiO_2 layer. Both of these models were simulated using the finite-difference time-domain method on Lumerical software (Lumerical Inc., USA).

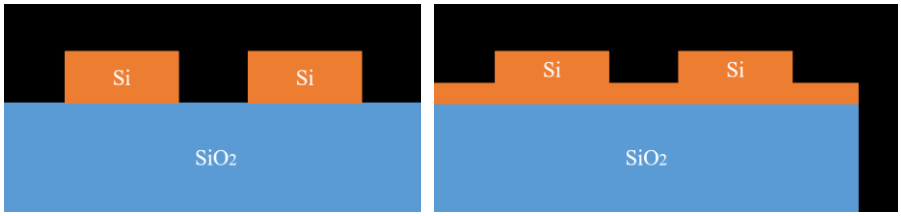

(a) **(b)**

Fig. 1. Two models of micro-ring resonator with differences in the dimension layer: (a) Model 1, ring resonator and signal waveguide are separate parts, (b) Model 2, the ultimate layer connected ring resonator and signal waveguide.

We simulated the two different configurations of a micro-ring resonator with several modified dimensions, as can be seen in Table 1, to investigate them. Both models were simulated for the same propagation light wavelength around 1500 nm, which the light of this wavelength interact well with the analyte [11]. The length of gap, ring radius, and waveguide width of Model 1 and Model 2 were modified with the same dimensional variation of 50-140 nm, 4.5-12 µm, and 450-550 nm, respectively. The difference between Model 1 and Model 2 is the structure of the Si layer. For Model 1, the etching depth of Si layer is 0 nm, whereas for Model 2, the etching depth varied from 40 to 120 nm. These two different models are created to observe the characteristics of the optimum values of FSR and Q-factor.

Table 1. The dimensions of micro-ring resonator.

	Symbol	Unit	Model 1	Model 2
Wavelength	λ	nm	1400-1600	1400-1600
Waveguide height	h	nm	220	100-180
Etching depth	H	nm	0	40-120
Total Si layer height	-	nm	220	220
Length of gap	g	nm	50-140	50-140
Ring radius	r	µm	4.5-12	4.5-12
Waveguide width	W	nm	450-550	450-550

3. Results and Discussion

The simulation results obtained different FSR and Q-factor values, depending on the dimensions of micro-ring. Q-factor is the parameter of the micro-ring resonator to the sensitivity of micro-ring sensors. The Q-factor of a given device is a measure of the resonant photon lifetime within a microstructure (the higher the Q-factor, the longer the lifetime) and Q-factor is corrected for the number of times a photon is re-circulated and allowed to interact with the analyte [12]. Therefore, larger Q-factor means higher sensitivity. The FSR is the distance

between two resonance peaks adjacent [13]. A higher FSR value gives information about larger detection limit. This is because the distance between the two maximum resonance peaks is wider hence more wavelength shift can be distinguished. The explanation of the result of the effect of the dimensions on the FSR and the Q-factor value is described in the following.

3.1. Waveguide width

Figure 2 shows the effect of waveguide width variation on the values of FSR and Q-factor for Model 1 (Fig. 2(a)) and Model 2 (Fig. 2(b)). The waveguide width varied from 450 to 550 nm, whereas the other parameters were controlled to have a fixed dimension of 50 nm gap and 4.5 µm ring radius for both models. The etching depth of Model 1 is 0 nm, so that the waveguide height is 220 nm, whereas the etching depth and waveguide height of Model 2 are 40 and 180 nm, respectively.

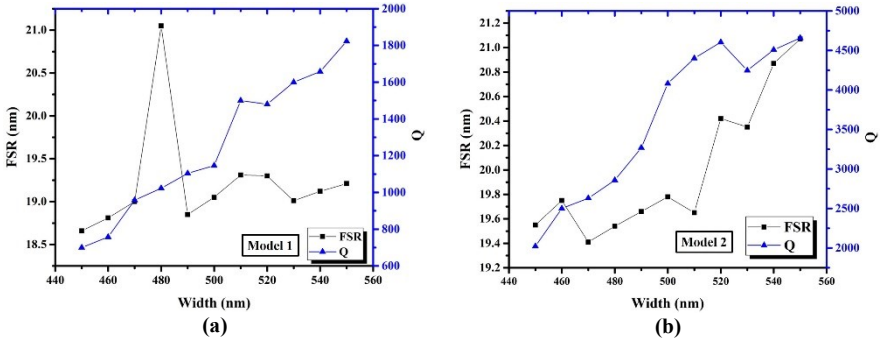

Fig. 2. The waveguide width optimization of micro-ring resonators for FSR and Q-factor results in: (a) Model 1 and (b) Model 2.

The FSR values of Model 1 and Model 2 relatively increase with respect to the increasing waveguide width. The FSR value of Model 1 increases from 18.66 to 21.04 nm, whereas the FSR value of Model 2 increases from 19.41 to 21.07 nm. The waveguide widths for the optimum value of FSR for Model 1 and Model 2 are 480 and 550 nm, respectively. Larger FSR means that more signal can be accommodated in one channel at once. However, it must be remembered that the width cannot be too narrow or too wide [14, 15]. If the waveguides are too wide, then the evanescent waves could not extend more into the outside of the waveguides to interact with the analyte. Hence, the evanescent waves cannot create a larger impact on modifying the refractive index effective of waveguides and so the sensitivity will be decreased. On the other hand, we also need to keep in mind that the waveguides cannot be too narrow due to an increase of the propagation loss.

The Q-factor value is also affected by the change on the waveguide width dimension, which leads to the increasing value of Q-factor respectively to the increasing value of waveguide width. This result was in agreement with that of the previous study conducted by Mulyanti [16]. The Q-factor in Model 2 has a higher value than Model 1. In Model 1, the value of the Q-factor increased from 712.94 to 1832.21 when the width values were between 450 and 550 nm, whereas in Model 2, the value of the Q-factor is in the range of 2024.35-4667.98. Both

Models 1 and 2 have the same waveguide width of 550 nm to obtain the optimum value of Q-factor. The loss in micro-ring resonator can be reduced by using wider waveguides for better optical confinement, which provides a higher Q-factor value by sharpening the resonance peak. Mahmudin et al. [17] mentioned that, however, the waveguides should not be too wide [17].

3.2. Gap

The FSR and Q-factor values of Model 1 and Model 2 are observed in Fig. 3(a) and Fig. 3(b), respectively, by altering the length of the gap. The gap varied from 50 to 140 nm for both models. The other parameters of Model 1 and Model 2 were set to have a fixed value. For Model 1, the values of the ring radius, waveguide width, waveguide height, and etching depth are 4.5 μm, 450 nm, 220 nm, and 0 nm respectively whereas for Model 2 are 4.5 μm, 450 nm, 180 nm, and 40 nm, respectively.

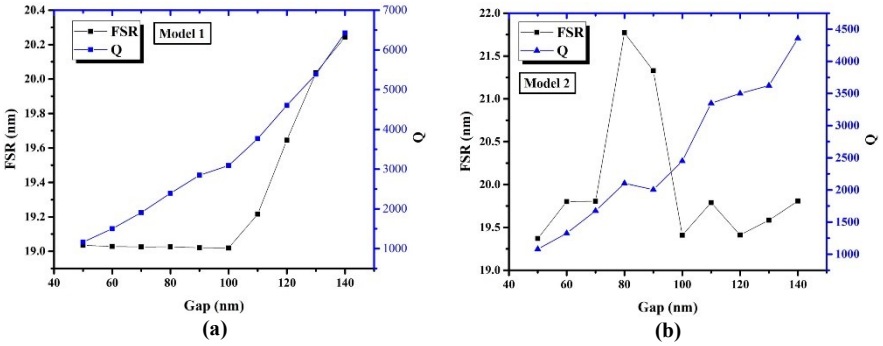

Fig. 3. The gap optimization of micro-ring resonators for FSR and Q-factor results in (a) Model 1 and (b) Model 2.

The FSR value of Model 1 is constantly around 19.00 nm for the gap length variation of 45 nm to 100 nm then gradually increases with linear-like pattern with sharp gradient for the gap length variation of 110 to 140 nm with the highest FSR value of 20.24 nm. The FSR value of Model 2 increases to 21.30 nm when the gap length is 80 nm and decreases when the gap length value varies from 90 to 140 nm. Theoretically, the reason why high FSR value occurs in Model 2 for a gap of 80 and 90 nm is that the reference gap is able to reduce the coupling scattering, hence optimizing the value of FSR [18]. The change of the gap values also affects the value of the Q-factor. The values of Q-factor in Model 1 and Model 2 are increasing alongside the increasing gap length. The Q-factor value of Model 1 varies from 1157.49 to 6456.72, whereas that of Model 2 varies from 1081.36 to 4361.94. Hence, we can see that the Q-factor value of Model 1 is higher than that of Model 2. The optimum FSR and Q-factor values of Model 1 are obtained with a gap length of 140 nm, whereas for Model 2, the optimum FSR value is obtained with a gap length of 80 nm.

3.3. Ring radius

We observed the correlation between the ring radius and values of FSR and Q-factor in the two types of the different configurations of micro-ring resonator,

namely, Model 1 (Fig. 4(a)) and Model 2 (Fig. 4(b)). The ring radius for Model 1 and Model 2 varied from 4.5 to 12 μm, whereas the other parameters, such as waveguide width, waveguide height, gap length, and etching depth, are set to be constant. We set the waveguide width and gap length to be 220 and 50 nm, respectively, for both Model 1 and Model 2. The difference between Model 1 and Model 2 is the etching depth. Model 1 has an etching depth of 0 nm; hence, the waveguide height is 220 nm. Model 2 has an etching depth of 40 nm; hence, the waveguide height is 180 nm.

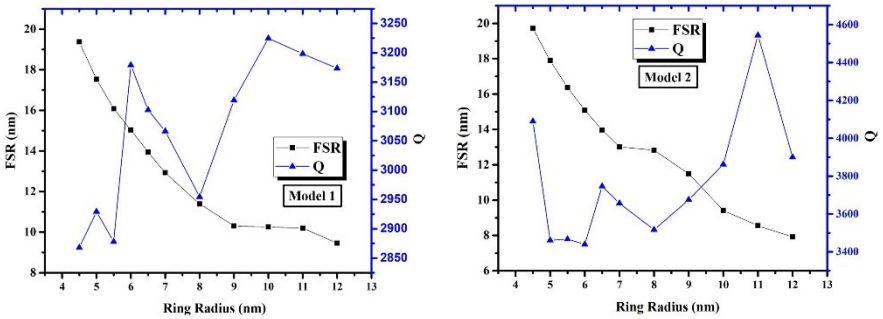

Fig. 4. The ring radius optimization of micro-ring resonators for FSR and Q-factor results in (a) Model 1 and (b) Model 2.

The increase of the ring radius leads to the decrease of the FSR value for both Model 1 and Model 2. By altering the ring radius between 4.50 and 12 μm, the FSR value decreases in Model 1 and Model 2, respectively, between 19.43-9.47 nm and 19.78-7.90 nm. This result corresponds to that of the previous study conducted by Mulyanti [19] and Aziz et al. [20]. The FSR values affected by the ring radius due to the FSR as the width of the pass band area generate by the filtering of the micro-ring resonator [21]. Thus, to obtain a micro-ring resonator with a high FSR value, the radius value should be smaller. However, this is more difficult to do for fabrication due to the limitations of the tools used.

The Q-factor values for both models were irregular. But, the value of the Q-factor in Model 2 was higher than that in Model 1. The changes of the radius value between 4.5 and 12 μm enabled Model 1 to have a maximum Q-factor of 3228.15 nm and minimum Q-factor of 2865.49 nm, whereas Model 2 has a maximum Q-factor of 4554.90 and a minimum Q-factor of 3440.27. The value of the Q-factor was influenced by the radius value, but the change of the Q-factor value was not linier along with the increases of the radius value [22], because the radius value depends on closed or widened the resonance value. Thus, the accuracy of the sensor adjusted to the radius micro-ring value.

3.4. Etching depth

We investigate the optimized values of FSR and Q-factor as shown in Fig. 5 by altering the etching depth of the Si layer in Model 2. The etching depth varied from 40 to 120 nm while the total Si layer height was fixed at 220 nm. The ring radius, waveguide width, and gap length were fixed at 4.5 μm, 450 nm, and 50 nm, respectively.

The Q-factor increased relatively when the entire surface of the micro-ring resonator was etched. This is because the Q-factor is influenced by the distance formed from the etching result. Thus, the gap is formed, producing the Q-factor value for the micro-ring [19]. The etching depth optimization is obtained on an etching depth of 60 nm with the Q-factor and FSR values at 7184.16 and 20.75 nm, respectively.

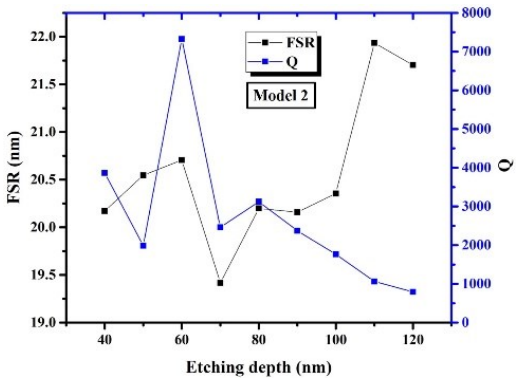

Fig. 5. Etching depth optimization for Model 2.

3.5. FSR and Q-factor values based on the optimized parameters

We obtained the optimized parameters based on the optimization of micro-ring resonator parameters for Model 1 and Model 2. From the previous parameter, optimization results show that Model 1 has the optimum value when using the dimension of the micro-ring resonator of waveguide width, gap, and ring radius at 480 nm, 140 nm, and 4.50 μm, respectively. Model 2 has the optimum value in the dimension of the micro-ring resonator when setting waveguide width, gap, ring radius, and etching depth at 550 nm, 80 nm, 4.5 μm, and 60 nm, respectively.

Table 2 shows the comparison between the optimum FSR and Q-factor values for Model 1 and Model 2. The FSR values of Model 1 and Model 2, which has been optimized for all the parameters, provide FSR value nearly 20 nm, which is sufficient for the purpose of biosensors because it has a relatively large FSR [21], whereas for the Q-factor value, Table 2 shows that both Model 1 and Model 2 provide higher Q-factor values compared with the rest, whereas Model 1 has a higher Q-factor value than Model 2. According to Chalyan et al. [23], larger Q-factor is needed for better sensitivity of micro-ring resonator-based sensor.

The originality of this study is that it explores the influences of the addition of etching depth to the configuration of micro-ring resonator on Model 2 by comparing the values of FSR and Q-factor in Model 1 and Model 2. Based on this study, it has been known that both models provide FSR values near 20 nm, which shows that both models have a fine FSR for sensors and also the addition of etching depth does not significantly affect FSR. As for the value of Q-factors, Model 1 has larger value than Model 2 with the difference about 3000. These results shows that Model 1 has better sensitivity and also the addition of etching depth will reduce the performance of micro-ring resonator sensors by decreasing its sensitivity.

Table 2. Optimize values of FSR and Q-factor for Model 1 and Model 2.

Parameter Optimization	Model 1		Model 2	
	FSR (nm)	Q-factor	FSR (nm)	Q-factor
Waveguide width	21.05	1823.08	21.07	4657.69
Gap length	20.24	6425.87	21.77	4358.491
Ring radius	19.37	3224.63	19.72	4543.695
Etching depth	-	-	21.94	7184.16
Every parameter optimized	19.61	10559.10	20.73	7294.51

4. Conclusions

Both models of the micro-ring resonator have high values of FSR and Q-factor, which depend on the micro-ring dimension. The simulation has been conducted by changing some dimensions in both models, including the waveguide width, gap, radius, and etching depth. The results show that Model 1 has the optimum values of FSR and Q-factor of 19.61 and 10559.10 nm, respectively, whereas Model 2 has the optimum values of FSR and Q-factor of 20.73 and 7294.51 nm, respectively. We also found that the addition of etching depth could produce higher FSR value, but unfortunately, it can reduce the value of Q-factor. However, both models successfully produced sufficient values of FSR and Q-factor; hence, both Model 1 and Model 2 can be used as sensors with good sensitivity.

Acknowledgements

We gratefully acknowledge to Directorate of Research and Community Service, Ministry of Research, Technology and Higher Education, the Republic of Indonesia for financial supporting through the grant of Penelitian Terapan Unggulan Perguruan Tinggi.

Nomenclatures

g	Length of micro-ring gap, m
H	Total of upper layer, m
h	Etching depth, m
r	Ring radius, m
W	Waveguide width, m

Greek Symbols

λ	Wavelength, m.

Abbreviations

FSR	Free Spectral Range
Q-factor	Quality factor
SiO_2	Silicon oxide

References

1. Zhu, L.; and Zeng, W. (2017). Room-temperature gas sensing of ZnO-based gas sensor : A review. *Sensors Actuators A. Phys*, 267(1), 242-261.

2. Chengyang, X.; Jingque, W.; Chao, L.; Yonghua, W.; Danfeng, C.; and Wendong, Z. (2013). Research on optical biological sensor used as quantitative analysis of glucose. *Proceeding of the annual IEEE International Conference on Nano/Micro Engineered and Molecular System*. Suzhou, China, 953-956.
3. Donzella, V.; Sherwali, A.; Flueckiger, J.; Grist, S. M.; Fard, S. T.; and Chrostowski, L. (2015). Design and fabrication of SOI micro-ring resonators based on sub-wavelength grating waveguides. *Optics Express,* 23(4), 4791-4803.
4. Wright, J. (2010). High Quality Factor Silicon Nitride Ring Resonators for Biological Sensing. *Electrical Engineering*, 1-24.
5. Amiri, I.S.; Ariannejad, M.M.; Ghasemi, M.; Naraei, P.; Kouhdaragh, V.; Seyedi, S.A.; Ahmad, H.; and Yupapin, P. (2017). Simulation of microring resonator filters based ion-exchange buried waveguide using nano layer of graphene. *Journal of Optics*, 46(4), 506-514.
6. Tao, J.F.; Cai, H.; Wu, J.; Tsai, J.M.; Zhang, Q.X.; Lin, J.T.; and Liu, A.Q. (2013). Optical wavelength signal detector via tunable micro-ring resonator for sensor applications. *Proceedings of the 26th IEEE International Conference on Micro Electro Mechanical Systems (MEMS)*. Taipei, Taiwan, 500-503.
7. Bogaerts, W.; Fiers, M.; and Dumon, P. (2013). Design challenges in silicon photonics. *IEEE Journal of Selected Topics in Quantum Electronics*. 20(4), 1-8.
8. Guider, R.; Gandolfi, D.; Chalyan, T.; Pasquardini, L.; Samusenko, A.; Pederzolli, C.; Pucker, G.; and Pavesi, L. (2015). Sensitivity and Limit of Detection of biosensors based on ring resonators. *Sensing and Bio-Sensing Research*, 6, 99-102.
9. Haroon, H.; Shaari, S.; Menon, P.S.; Mardiana, B.; Hanim, A.R.; Arsad, N.; Majlis, B.Y.; Mukhtar, W.M.; Abdullah, H. (2012). Design and Characterization of Multiple Coupled Microring Based Wavelength Demultiplexer in Silicon-on-Insulator (SOI). *Journal of Nonlinear Optical Physics & Materials*, 21(1), 1-8.
10. Luchansky, M.S; and Bailey, R.C. (2011). High-Q optical sensors for chemical and biological analysis. *Analytical Chemistry*, 84(2), 93-821.
11. De Vos, K.; Bartolozzi, I.; Schacht, E.; Bienstman, P.; and Baets, R. (2007). Silicon-on-Insulator microring resonator for sensitive and label-free biosensing. *Optics Express*, 15(12), 7610-7615.
12. Ganjalizadeh, V.; Veladi, H.; and Yadipour, R. (2014). A novel pressure sensor based on optofluidic micro-ring resonator. *International Conference on Optical MEMS and Nanophotonics*. Glasgow, UK, 133-134.
13. Zakaria, M.; Hasanah, L.; and Suhendi, E. (2017). Modeling and simulation of microring resonator with clutter variations as sensor and telecommunication device. *In Wahana Fisika*. Bandung, Indonesia, 57-66.
14. Chao, C.Y.; and Guo, L.J. (2006). Design and optimization of microring resonators in biochemical sensing applications. *Journal of Lightwave Technology*. 24(3), 1395-1402.
15. Jimenez, J.J.; and Guijarro, J.J. (1973). Experimental Q factors of three types of microstrip resonators. *Revue de Physique Appliquée*, 8(3), 279-282.

16. Mulyanti, B.; Ramza, H.; Pawinanto, R.E.; Rahman, J.A.; Ab-Rahman, M.S.; Putro, W.S.; Hasanah, L; and Pantjawati, A.B. (2017). Micro-ring resonator with variety of gap width for acid rain sensing application: preliminary study. *Journal of Physics: Conference Series*. 852, (1), 012043.
17. Mahmudin, D.; Estu, T.T.; Daud, P.; Hermida, I.D.P.; Sugandi, G.; Wijayanto, Y.N.; Menon, P.S.; and Shaari, S. (2015). Sensitivity improvement of multipath optical ring resonators using silicon-on-insulator Technology. *IEEE Regional Symposium on Micro and Nanoelectronics (RSM)*. Kuala Terengganu, Malaysia, 293-296.
18. Van, V. (2017). *Optical Microring Resonators Theory, Techniques, and Applications*. Boca Raton: Taylor & Francis Group.
19. Mulyanti, B.; Menon, P.S.; Shaari, S.; Hariyadi, T.; Hasanah, L.; and Haroon, H. (2014). Design and optimization of coupled Microring Resonators (MRRs) in silicon-on-insulator. *Sains Malaysiana*. 43(2), 247-252.
20. Aziz, N.N.A.; Haroon, H.; and Razak, H. (2016). Compact optical filter based on microring resonator. *ARPN J. Eng. Appl. Sci.*, 11(5), 3230-3323.
21. Guo, J.; Shaw, M.J.; Vawter, G.A.; Hadley, G.R.; Esherick, P.; and Sullivan, C.T. (2005). High-Q microring resonator for biochemical sensors High-Q microring resonator for biochemical sensors. *Integrated Optics: Devices, Materials, and Technologies IX*. 5728, 83-92.
22. Vahala, K.J. (2003). Optical microcavities. *Nature*. 424, 839-846.
23. Chalyan, T.; Gandolfi, D.; Guider, R.; Pavesi, L.; Pasquardini, L.; Pederzolli, C.; Samusenko, A.; and Pucker, G. (2015). Characterization of SION microring resonators for biosensing applications. *In The International Conference on BioPhotonics (BioPhotonics)*. Florence, Italy , 1-4.